JGR Space Physics

RESEARCH ARTICLE
10.1029/2021JA030042

Disconnection and Reconnection in Plasma Bubbles Observed by OI 630 nm Airglow Images From Cariri Observatory

A. J. Carrasco[1,2], I. S. Batista[2], C. M. Wrasse[3], H. Takahashi[3], and A. A. Pimenta[2]

[1]Department of Physics, Los Andes University, Mérida, Venezuela, [2]Heliophysics, Planetary Science and Aeronomy Division, National Institute for Space Research (INPE), São José dos Campos, Brazil, [3]Space Weather Division, National Institute for Space Research (INPE), São José dos Campos, Brazil

Key Points:

- First observations of disconnection and reconnection of plasma bubbles were obtained in the Cariri observatory
- The detachment first consists of the separation of a part of the bubble to be later captured by a neighboring bubble
- The occurrence rate of the phenomenon of disconnection and reconnection between adjacent bubbles is very low, and it occurs during-low, medium, and high solar fluxes

Correspondence to:

A. J. Carrasco,
layerf2@gmail.com

Citation:

Carrasco, A. J., Batista, I. S., Wrasse, C. M., Takahashi, H., & Pimenta, A. A. (2022). Disconnection and reconnection in plasma bubbles observed by OI 630 nm airglow images from Cariri observatory. *Journal of Geophysical Research: Space Physics*, *127*, e2021JA030042. https://doi.org/10.1029/2021JA030042

Received 10 DEC 2021
Accepted 20 APR 2022

Author Contributions:

Conceptualization: A. J. Carrasco, I. S. Batista, C. M. Wrasse, H. Takahashi, A. A. Pimenta
Methodology: A. J. Carrasco
Writing – original draft: A. J. Carrasco, I. S. Batista
Writing – review & editing: A. J. Carrasco, C. M. Wrasse, H. Takahashi, A. A. Pimenta

Abstract We use OI 630 nm airglow images obtained with the All-sky imager installed at São João do Cariri (7.4°S, 36.5°W) to report the very rare phenomenon of disconnection and reconnection between adjacent plasma bubbles. We report here for the first time observations of the phenomenon at Cariri. These observations show that the phenomenon is independent of the solar flux and occurs between September and December in the Brazilian sector. The phenomenon consists first in separating a part of the bubble followed by its capture by other adjacent bubbles via electrostatic potential fields. Statistically, the phenomenon is of very low occurrence and its probability varies between 1/120 and 1/165 per year, and on certain occasions it is zero.

1. Introduction

Plasma bubbles are density irregularities or plasma depletions often occurring in the nighttime ionosphere after sunset at low latitudes and near the magnetic equator. These ionospheric plasma depletions or equatorial plasma bubbles, sometimes called equatorial spread-F, are a phenomenon related to the collisional Rayleigh-Taylor instability mechanism. Generally, equatorial plasma bubbles grow up from the bottom side to the upper F layer. While moving upward, the equatorial plasma bubbles can extend hundreds of kilometers along magnetic flux tubes in both hemispheres and often reach the equatorial ionization anomaly crest (Abdu et al., 2009; Batista et al., 2008; Sobral et al., 2009). Furthermore, the study of the Rayleigh-Taylor instability and equatorial plasma bubbles is relevant to understanding and modeling ionospheric plasma physics. All-sky imaging technique have been extensively used to study the ionospheric irregularities, using nightglow emissions at different wavelengths such as OI 630.0 and 557.7 nm. The dark patches in optical data of OI 630.0 nm emission reflect the depletion in plasma density compared to the background plasma density of the ionospheric bottom side F region, constituting the signature of equatorial plasma bubbles. The Cariri database constituted of almost 20 years of observations has been used in several works to study the characteristics of gravity waves and the bifurcation mechanism of the plasma bubbles (Carrasco et al., 2020; Medeiros et al., 2004; Paulino et al., 2016; Takahashi et al., 2005; Wrasse et al., 2006).

Based on maps of total electron content (TECMAP) over the South American continent, Takahashi et al. (2015) and Barros et al. (2018) observed periodically spaced bubble structures that were formed at the magnetic equator between 600 and 800 km of zonal distance and extending along magnetic flux tubes in both hemispheres. They interpreted that the periodic form of plasma bubbles may suggest a seeding process related to the solar terminator passage in the ionosphere and that the distance between successive plasmas bubbles is associated with the zonal drift velocity of the bubble. Barros et al. (2018) revealed that the latitudinal extension of the plasma bubbles over South America could reach values of 2,000 km for January, February, November, and December. Additionally, Barros et al. (2018) showed that for the period 2012–2016, the zonal drift velocity of the bubbles observed over Cariri varies between 100 and 150 m/s respectively. The nonlinear dynamic of ionospheric plasma bubbles leads to complex structures such as bifurcation, disconnection, and reconnection as confirmed by observations of airglow images. The bifurcation process is the division of one channel into two in a plasma bubble that grows vertically. In the progress of time, several branches can emerge in the plasma bubble as confirmed by observations and modeling. Recently, Carrasco et al. (2020) studied the bifurcation process of equatorial plasma bubbles using the PBM2D (Plasma Bubble Model in two Dimensions) code and they found that the bifurcation mechanism is controlled by the polarization electric fields inside the bubble. According to their numerical simulations, the bifurcation is initiated once the head of the plasma bubble has passed the peak of the F-layer and the maximum of the vertical component field (positive) is very close to the minimum value of the zonal field in the

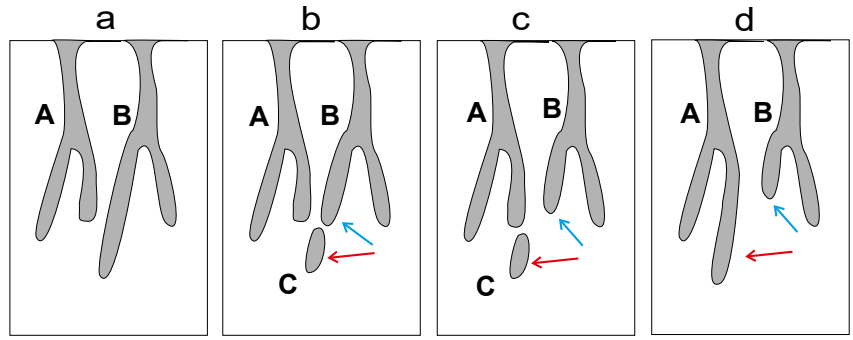

Figure 1. Schematic representation of a sequence of airglow images cartoons toward the southern hemisphere. The figure shows the disconnection and reconnection between adjacent bubbles.

middle part of the bubble. They also showed that the vertical electric field is bipolar inside the bubble, and their numerical results were supported by electric field measurements reported by Aggson et al. (1996). As it is already well known, the plasma bubble develops, initially at the magnetic equator, grows upward and extends in latitude. The phenomenon of disconnection and reconnection has been observed to occur in both magnetic hemispheres (Chian et al., 2018; Gurav et al., 2019; Narayanan et al., 2016a, 2016b). The phenomenon consists first of the separation of part of the bubble followed by its capture by a neighboring bubble via electrostatic potential fields. It has also been reported that the reconnection process can occur between adjacent plasma bubbles without detachment of parts, known as the merging process (Huba et al., 2015). Some efforts have been made to understand this phenomenon.

Based on the work of Huang and Kelley (1996), Sahai et al. (2006) suggested that the observed detached plasma bubble structures, from one of the bifurcated branches, are possibly associated with the development of non-homogenous vertical plasma drift (the upper part either moving faster or slower than the lower part) due to a non-homogeneous zonal electric field inside the bubble. Laakso et al. (1994) suggested that detachment of parts occurs when the plasma bubble, during its growth, is subjected to two vertical drifts in opposite directions. However, they did not show observations of airglow images that support their theory. More details of these two hypotheses are given in the following sections. The phenomenon of detachment or disconnection is an important part of the branching process of plasma bubbles. Conventionally, the scientific method is used as a verification mechanism for a hypothesis or conjecture that attempts to explain observations of nature.

In this work we present a study of the occurrence of the phenomenon of disconnection and reconnection between adjacent plasma bubbles for different levels of solar flux using observations obtained by the All-sky imager installed at Cariri. These observations of disconnection/reconnection obtained in São João do Cariri have not been presented in any previous works. Additionally, the scientific method is applied to Laakso et al. (1994)'s hypothesis through observations of vertical plasma drift at the equator and the airglow images at the low latitude.

2. Theoretical Considerations

To illustrate the phenomenon of detachment and reconnection, Figure 1 shows a schematic representation of a sequence of airglow images' cartoons. Figure 1a shows the branches of two close bubbles. After a certain time we can see in Figure 1b the first disconnection (marked as C and indicated by the arrows). In Figure 1c the part C moves to the west side and in Figure 1d, reconnection occurs with one of the bifurcated branches of bubble A. This phenomenon has been observed and reported by Chian et al. (2018), Narayanan, Gurubaran, and Shiokawa (2016), Narayanan, Gurubaran, Shiokawa, et al. (2016) and Gurav et al. (2019). Some theories have been developed to explain the phenomenon. Huang et al. (2012) using Retterer's (2010) model, showed that during the evolution of equatorial plasma bubbles, the tilt of one plasma bubble might interfere with the growing channel of another adjacent plasma bubble, resulting in their merging. Using simulation, Huba et al. (2015) showed that the merging between neighboring plasma bubbles (without detachment of parts) could be related

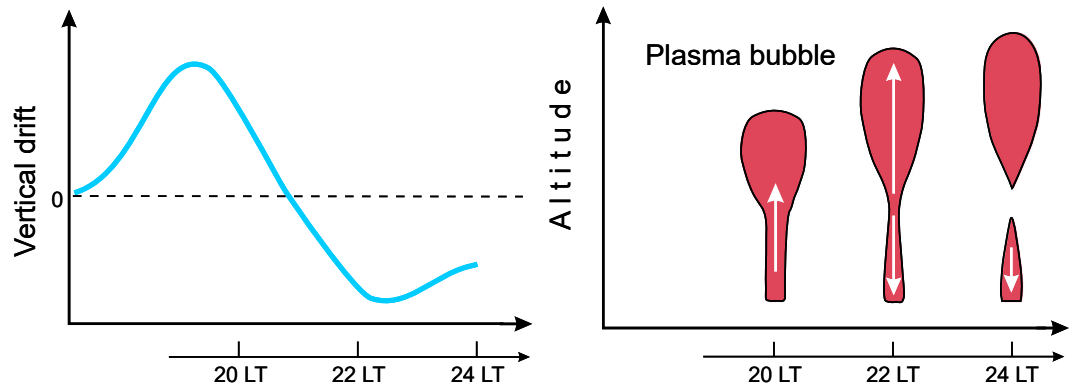

Figure 2. Schematic representation of the equatorial vertical drift (left panel) and the evolution sequence of a plasma bubble (right panel) based on the work of Laakso et al. (1994).

with the electrostatic potentials of the adjacent bubbles, and during reconnection high-speed plasma channels can develop in the merging process.

2.1. Theory 1: Detachment Caused by Non-Homogeneous Fields

Although we have a reasonable understanding of the factors that control daily and seasonal variations of plasma bubbles, the physics that control disconnection and reconnection is not well established. Sahai et al. (2006) suggested that the observed detached plasma bubble structures, from one of the bifurcated branches, are possibly associated with the development of a non-homogenous vertical plasma drift due to a non-homogeneous zonal electric field inside the bubble. Recently, Carrasco et al. (2020) showed, using simulation, the existence of non-homogeneous electric fields (zonal and vertical) inside the bubble varying in height and time. But their numerical simulations did not show detachment of structures. The reason could be attributed to the geophysical conditions selected for the simulation which differed from the present one. Yokoyama et al. (2014) showed by simulation detachment structure but the phenomenon was treated as a pinch-off, though the cause was not discussed in detail. The theory of detachment by non-homogeneous fields can be examined by numerical simulation but it is not the objective of the present work.

2.2. Theory 2: Detachment Caused by Opposite Vertical Drift

Based on measurements obtained by the San Marcos satellite, Laakso et al. (1994) suggests that detachment of parts occurs when the bubble in its vertical growth is subjected to two vertical drifts in opposite directions inside the bubble, but conditioned by the temporal variation of the equatorial plasma vertical drift of background. However, they did not present all-sky images to support their conjecture. This hypothesis is illustrated in Figure 2. According to this figure the plasma drifts upward all over the plasma bubble channel during the early evening hours. After ~21:00 LT (time of reversal of the vertical drift from positive to negative), the background zonal electric field turns westward, leading to a downward flow in the lower parts of the channel. A simultaneous occurrence of the downdraft and updraft plasma can finally pinch the upper part of the bubble off. This means that the walls of the bubble appeared to be collapsing inward, causing the formation of a dead bubble (Aggson et al., 1992). Additionally, in the hypothesis, the phenomenon of the detachment of the upper part of the plasma bubble from the lower one is conditioned to the temporal variation of the equatorial plasma vertical drift of background. It is known from observations that an intensification in the vertical plasma drift before reverting to negative values, known as the prereversal enhancement occurs almost every night and its occurrence in time varies seasonally. Consequently, if the premise is correct, one should expect that the plasma bubbles in 630.0 nm airglow images also show a high percentage of detachment, every time that vertical drift of background changes from positive to negative before local midnight.

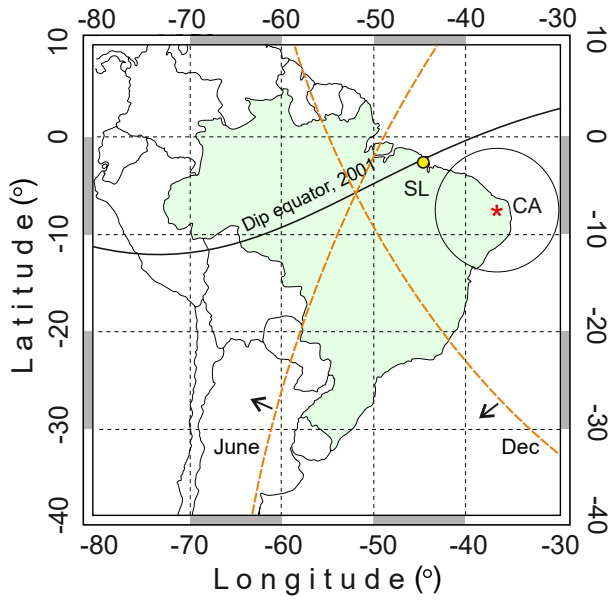

Figure 3. Map showing the location of São Luis (SL, digisonde) and Cariri (CA, all-sky imager). The circle indicates the field of view of the imager. The dashed orange lines represent the solar terminator for June and December, and the arrows indicate their direction of advance.

2.3. Theory 3: Detachment Caused by Shears in Zonal Drift

Based on observations of airglow images obtained from the Indian sector, Gurav et al. (2019) suggest that detachment of parts can be due to the large shears in zonal drift velocity with faster drifts in the top than in the bottom of the bubble. They also suggested that latitudinal variations in the zonal neutral wind may have contributed to changes in the plasma drifts.

3. Database

All-sky imaging technique have been extensively used to study the ionospheric irregularities by nightglow emissions at different wavelengths such as OI 630.0 nm and OI 557.7 nm from low latitude stations. The observation routine usually involved the acquisition of a few successive images using a particular filter for a prolonged duration depending on weather conditions.

Over the Brazilian territory, the first observational evidence of detached plasma bubble structures was reported by Sahai et al. (2006) in a sequence of airglow images in the OI 630 nm emission obtained at Brazópolis (22.5°S, 45.6°W) on 28 September 2002. Chian et al. (2018) extended the observational study of Sahai et al. (2006) and reported airglow images of neighboring plasma bubbles disconnecting and reconnecting. In the airglow images reported by Chian et al. (2018), they observed that the first disconnection occurs on the east side and after some time, the detached part is captured by an adjacent plasma bubble on the west side in the image.

In the present work, the OI 630 nm airglow images were obtained with the all-sky imager installed in São João do Cariri (7.4°S, 36.5°W), which is in operation since 2000 (Buriti et al., 2001). The results discussed herein are based on 3,900 nights of observations from 2001 to 2019, for a total of 2,012 nights with bubbles. During the period from 2001 to 2010 (~solar cycle 23) there were many nights without observations, due to either maintenance of the equipment or specific campaign mode operation (Paulino et al., 2016), while during the period 2011–2019 (solar cycle 24) the database is complete. Figure 3 shows the localization of São Luis (SL, 2.3°S, 44.0°W, digisonde) and São João do Cariri (CA, 7.4°S, 36.5°W, all-sky imager) in Brazil. The position of the magnetic equator is indicated by the solid black line. The black circle indicates the area covered by the all-sky imager for an emission altitude of 250 km. In the figure the solar terminator line (dashed orange) is shown for June and December and the arrows indicate the direction in which the terminator advances.

4. Observations: Occurrence of Bubbles

Figures 4a and 4b show the results for the frequency of occurrence (or the number of days) of plasma bubbles for each month of the years 2014 and 2019 (solar cycle 24). In the figure we can observe a minimum around June to July. The seasonal variation of occurrence is mainly due to the seasonal variation of the prereversal enhancement of the zonal electric field, which contributes to the development of the plasma bubble in altitude and latitude. Due to cyclical variations from one solar cycle to another, we can assume that the occurrence in solar cycle 23 (not shown here) is similar to that of solar cycle 24. In addition, in our database, there is a smaller number of observations of bubbles between 2001 and 2010 compared to the 2011–2019 period. Figure 4c shows the annual occurrence of plasma bubbles as a function of the annually averaged solar flux for the period 2012–2019, that is, the total number of days with plasma bubbles per year versus the annually averaged solar flux. The solid line represents the linear fit to the data. This figure also illustrates the linear dependence of the occurrence of bubbles with solar activity. The detection of bubbles in the all-sky field of view depends on its position concerning the magnetic equator. During low solar flux, the bubbles may be present at the equator (ionograms, spread-F) and not be observed by the all-sky at low latitude. This could partly explain the two lowest points in Figure 4c. In addition, the scatter of points is partly due to the different rates of increase with solar flux in the cycle and the magnetic activity effect.

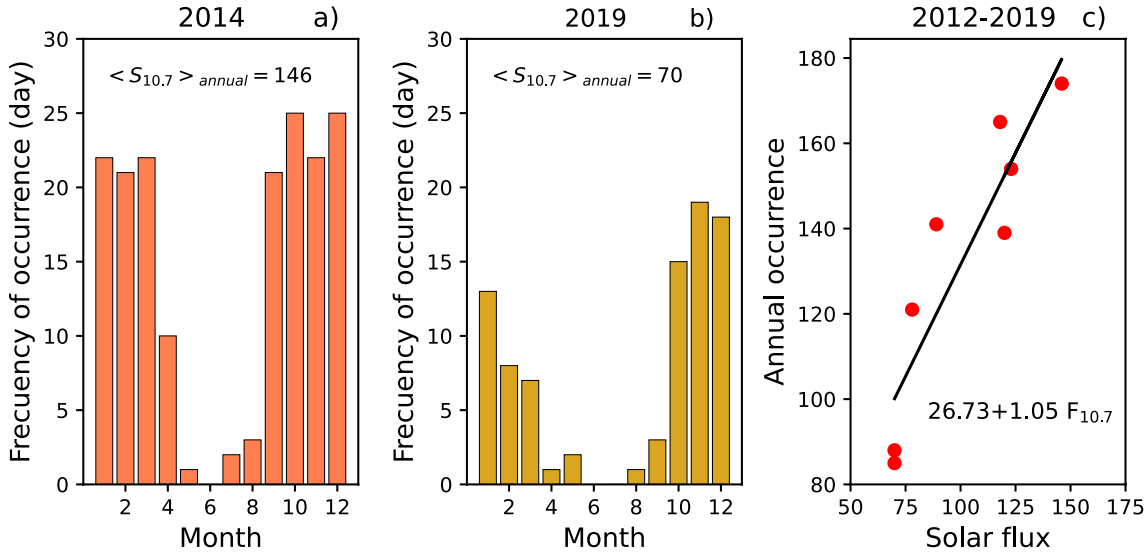

Figure 4. Frequency of occurrence of bubbles was plotted as a number of days for each month of the years 2014 and 2019, and the annual occurrence of bubbles as a function of average solar flux.

5. Observations: Plasma Vertical Drift

The plasma vertical drift of the ionospheric F region has been extensively measured for more than 50 years at the Jicamarca Radar Observatory, theoretically modeled by Heelis et al. (1974) and Batista et al. (1986) and empirically simulated by Scherliess and Feger (1999). In places where radars are not available, the vertical drift has been inferred from Digisondes measurements at the equator and low latitudes, using the method described by Bittencourt and Abdu (1981). Although conventional ionosonde measurements do not provide accurate plasma drift measurements most of the day, they precisely determine the vertical drifts evening reversal times. It is well known that the daytime equatorial F layer moves upward due to the vertical plasma drift ($\boldsymbol{E} \times \boldsymbol{B}$) generated by the eastward electric field induced by the E region dynamo. This electric field is reversed at night, also causing a reversal in the vertical drift to downward. Before its reversal, the electric field undergoes a rapid enhancement, giving rise to a pre-reversal maximum in drift velocity, which is believed to be caused by the buildup of the polarization electric field (F region dynamo field) that arises from the postsunset decrease in the E layer conductivity (Batista et al., 1986). The vertical plasma drift velocity is the most important parameter for the generation and development of plasma bubbles and the growth rate of the Rayleigh-Taylor instability depends on the vertical drift (Carrasco et al., 2014; Fejer et al., 1999). A higher equatorial vertical drift velocity (eastward electric field and pre-reversal peak) leads to a rapid development and great extension in the height and latitude of the plasma bubbles. Batista et al. (1986) showed that the seasonal effects on the occurrence time of the evening F region vertical drift pre-reversal peak are most pronounced in the months from June to August in the Brazilian sector. Fejer et al. (1991) showed that the pre-reversal peak velocity increases linearly with solar flux but decreases slightly with magnetic activity. The seasonal variation of the vertical drift at a given equatorial station is controlled by the magnetic declination angle and the seasonal variation of the sunset times at its magnetic conjugate E layers in both hemispheres (North-South). These seasonal changes are a consequence of the movement of the earth in its orbit around the sun, which causes changes in the declination of the solar terminator (day/night) concerning the local geographic meridian, varying from −23.44° to +23.44°, being close to zero in March and September. The meridional magnetic plane that passes through Cariri and Sao Luis stations tends to be aligned with the solar terminator, between the months of January–February and November–December respectively. From 2001 to 2015, São Luis can be considered an equatorial station. Figure 5a shows the vertical drift average monthly variation, around sunset over São Luis for quiet days (the year 2001). The figure shows that in general, the prereversal evening maximum has the highest amplitudes in the equinoxes and summer months. For the other years, 2002, 2003, etc. (not shown here), similar seasonal variation is observed. Figure 5b shows the vertical drift for only the days related to detachment events in the present study, which will be described in Section 6. The pre-reversal

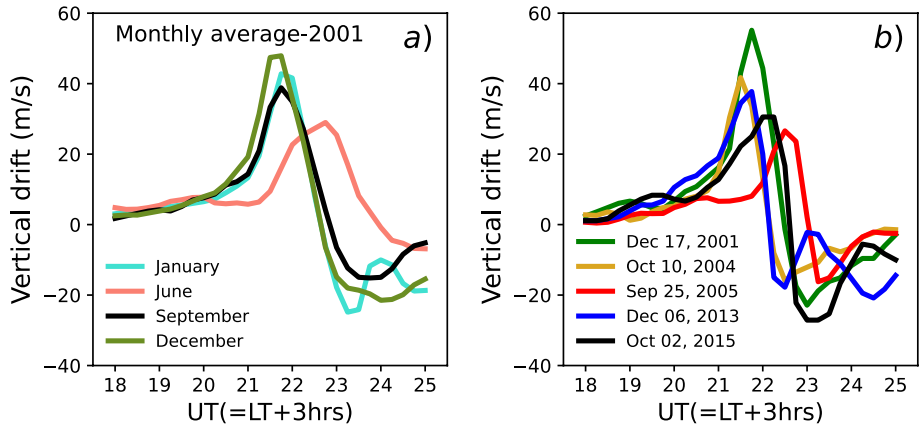

Figure 5. Average vertical drifts obtained at São Luis during 2001 and other vertical drifts for specific days.

maximum on 25 September 2005, could have been slightly affected by a magnetic storm, whose maximum negative of Dst (=−139) takes place on 11 September 2005, and the recovery phase took 14 days.

6. Observations: Disconnection and Reconnection

From 2001 to 2019, the magnetic inclination of Cariri varied from −19° to −25°, but the magnetic declination remained at −20°. A total of five events with detachment and reconnection were identified on the database of 3,900 nights of observation. In the following paragraph, a description of the identified events is given.

6.1. Event 1

Figure 6 shows the images acquired during the night of 17 December 2001 from Cariri. In Figures 6a and 6b, two closely spaced plasma bubbles, marked as A and B, are moving eastward with a zonal drift velocity of ∼97 m/s. The drift velocity was calculated using the method described in Arruda et al. (2006). From Figure 6d, it is possible to observe the separation of branch C from bubble B, indicated by the yellow arrow. An important feature noticed in this process of detachment is the capture of part C by plasma bubble A, as shown in Figure 6e, which is interpreted as a reconnection through electrostatic potentials between both parts. In Figure 6f, both parts (A + C) can be seen as a single bubble traveling at the same zonal drift velocity.

6.2. Event 2

Figure 7 shows the images obtained on the night of 10 October 2004, from Cariri. Figures 7a and 7b, show the branches of a bifurcated bubble marked as A and B, which moves eastward with a zonal drift velocity of ∼107 m/s. From Figure 7c, we can observe the initial phase of the separation of part C of branch B. From Figure 7d, it is clear to observe the reconnection of C with branch A through an inclined channel, indicated by the blue arrow. Figure 7e shows a better definition of the established reconnection.

6.3. Event 3

Figure 8 shows the airglow images on the night of 25 September 2005 from Cariri. Figures 8a–8f show a bifurcated bubble of narrow thickness, which moves eastward with a velocity of ∼81 m/s. The disconnection of part C of branch B occurs at 21:50:32 LT (yellow arrow) but at 21:56:54 LT, the detached part is captured by branch A, producing an increase in the length of branch A. The elapsed time between disconnection and reconnection is ∼6 min for this case.

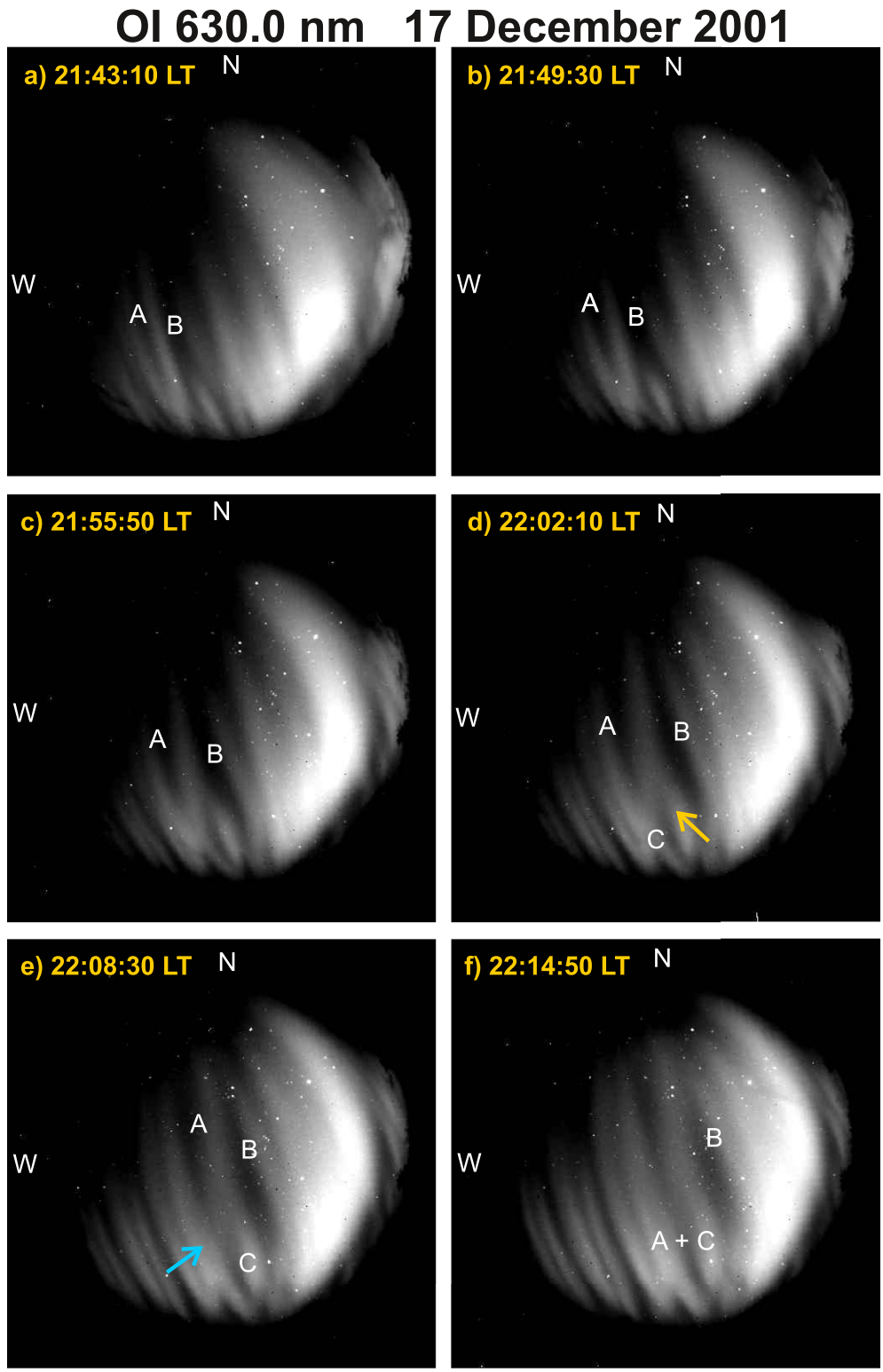

Figure 6. OI 630 nm images from Cariri on 17 December 2001.

6.4. Event 4

Figure 9 shows the airglow images on the night of 06 December 2013 from Cariri. In Figures 9a and 9b, two

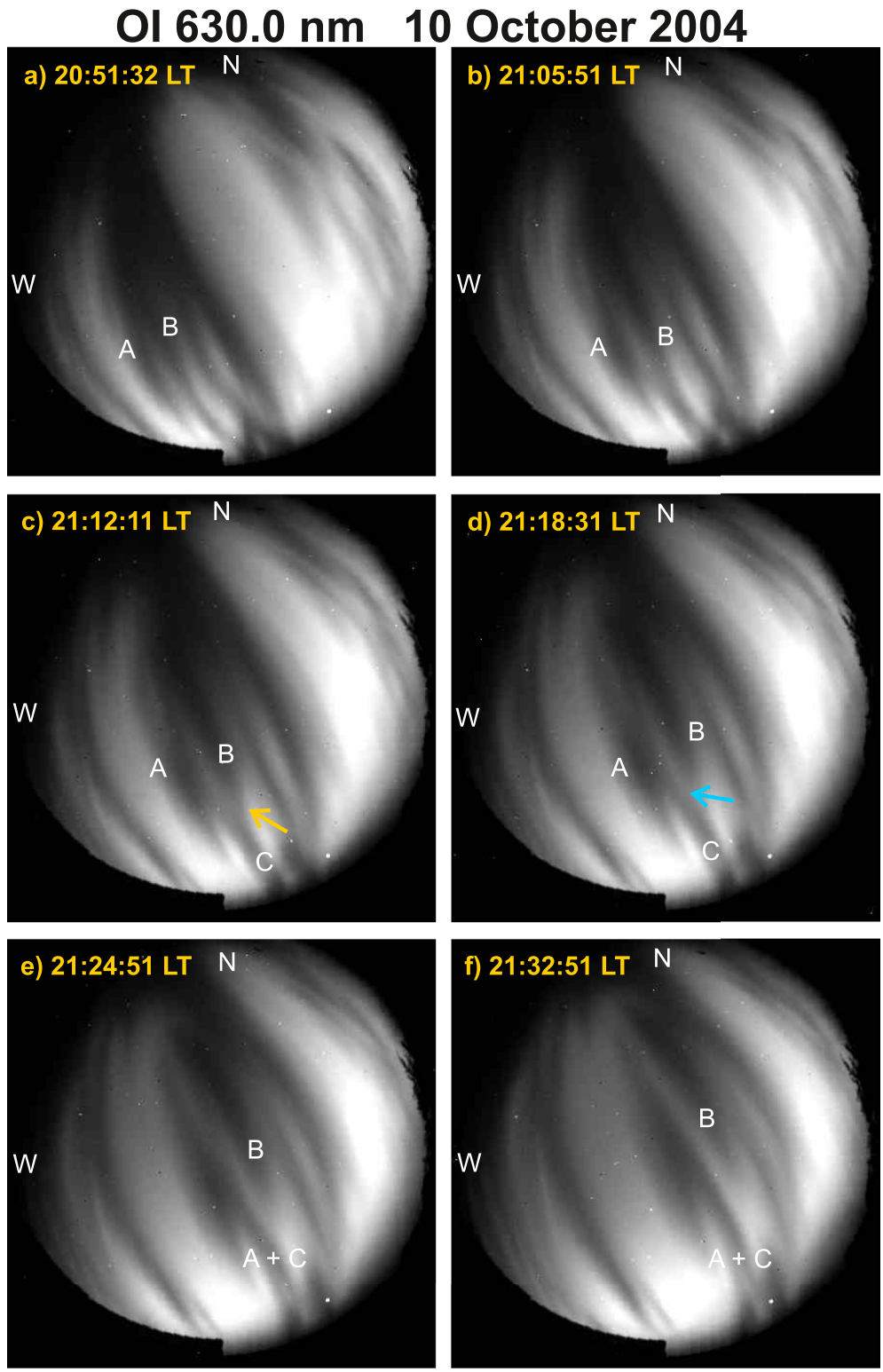

Figure 7. OI 630 nm images from Cariri on 10 October 2004.

closely spaced plasma bubbles of wide thickness, marked by A and B, move eastward with a velocity ~161 m/s. The disconnection of part C of branch B occurs at 21:55:21 LT (yellow arrow), but at 22:00:43 LT, the detached

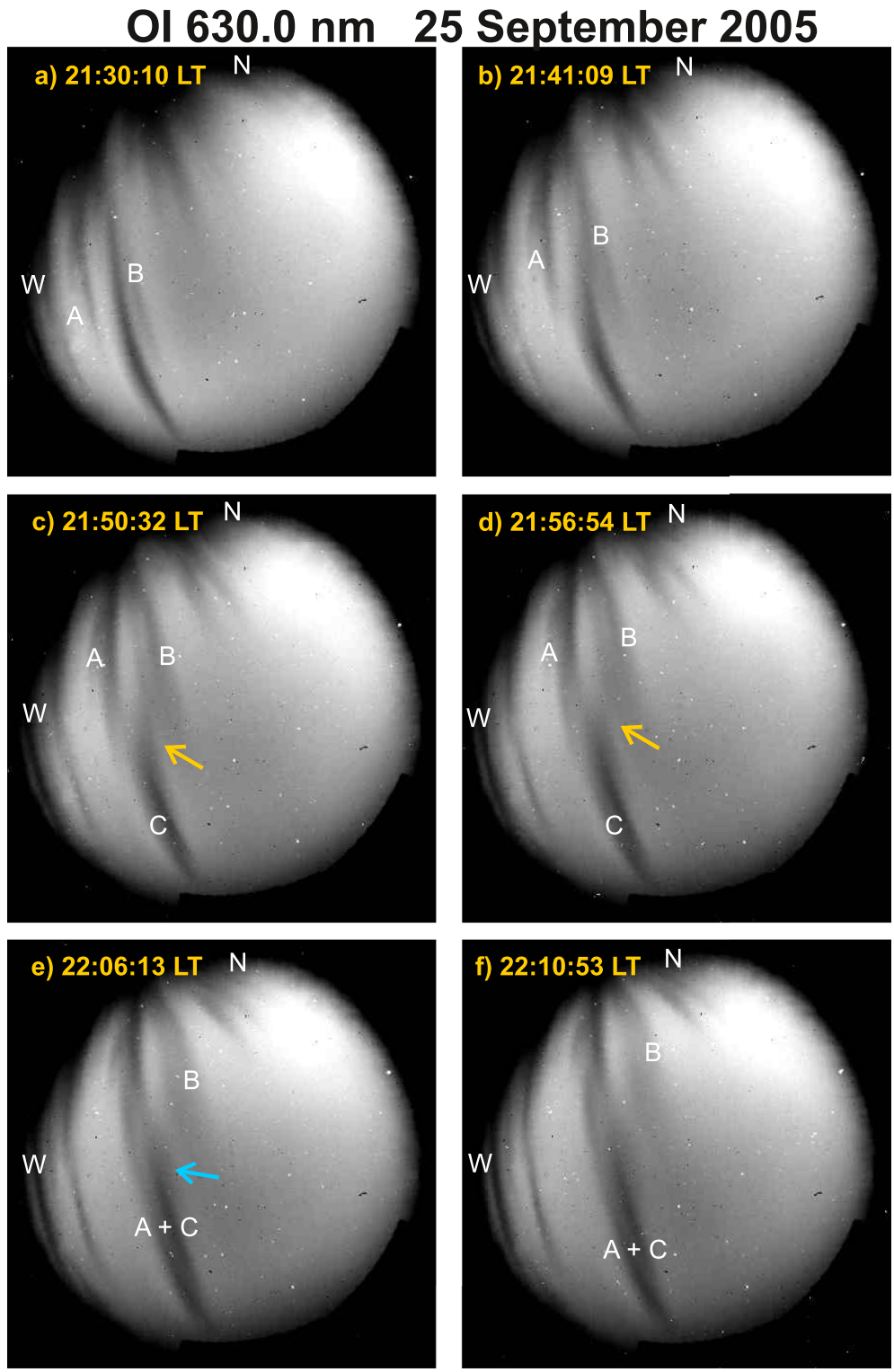

Figure 8. OI 630 nm images from Cariri on 25 September 2005.

part is captured by branch A (blue arrow). At the same time, it may be seen as the channel of reconnection between parts A and C. The elapsed time between disconnection and reconnection is ~5 min.

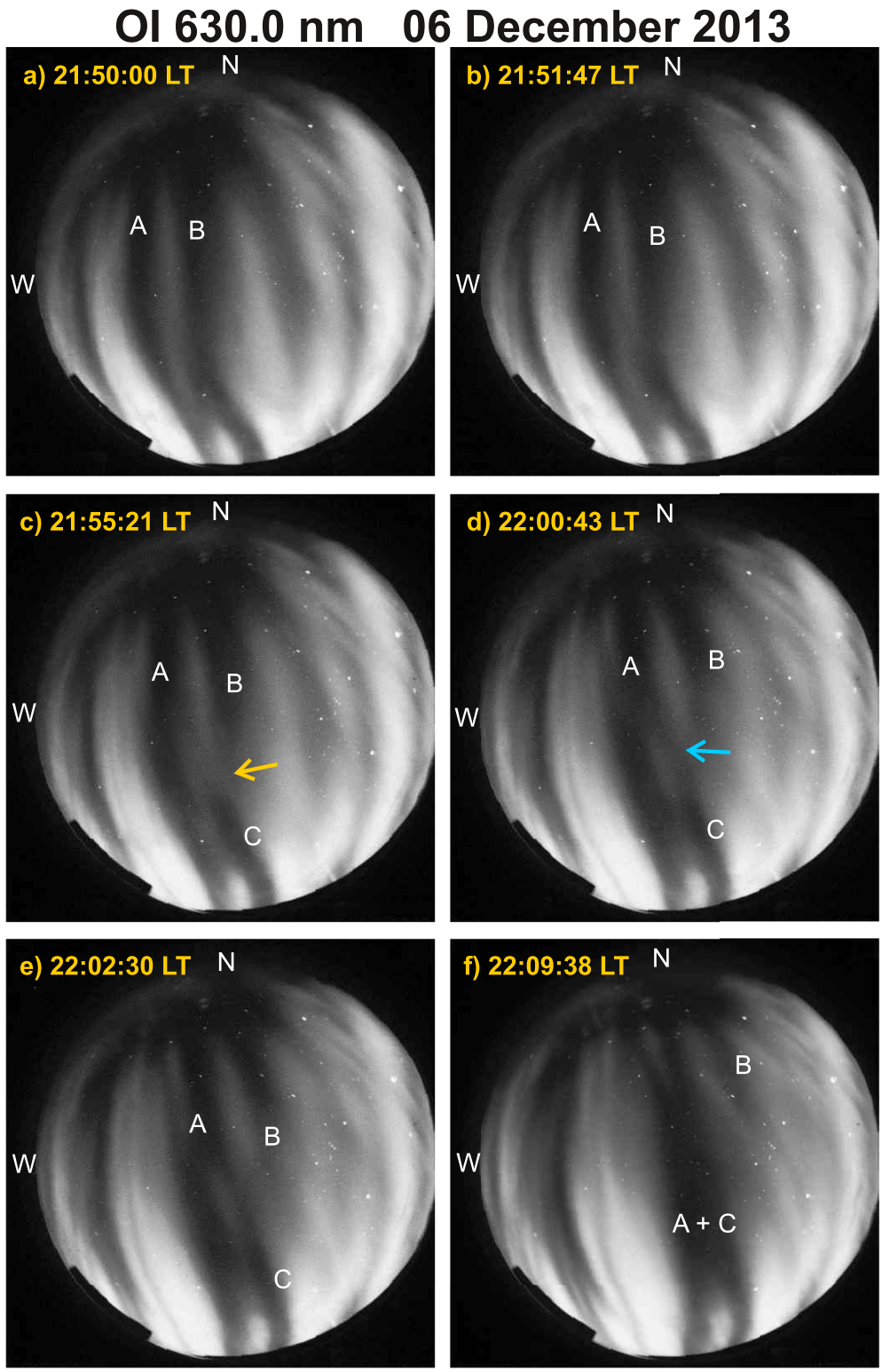

Figure 9. OI 630 nm images from Cariri on 6 December 2013.

6.5. Event 5

Figure 10 shows the airglow images on the night of 02 October 2015 from Cariri. Figures 10a–10f show two closely spaced plasma bubbles of wide thickness, marked by A and B, which move eastward with a velocity of ∼102 m/s. The disconnection of part C of arm B occurs at 22:41:24 LT (yellow arrow), but at 23:14:07 LT, the connection between arm A and part C seems to be established. In this event, we have no more images after 23:14:07 LT. When detachment occurs, the initial zonal distance between the branches from event 1 to event 5 were 155, 127, 102, 157, and 230 km respectively.

Table 1 shows the list of events of disconnection and reconnection observed in Cariri, together with other relevant parameters such as the detachment onset time (TimeD), the reconnection onset time (TimeR), the apex height, the Ap index and the solar flux at 10.7 cm (F10.7). The point of detachment in the airglow images was mapped to the equatorial magnetic plane to determine the apex height for each event. With only five cases available, it was not possible to determine the dependence of the apex height with solar flux, displacement of the magnetic equator, or some other geophysical parameter. The average pattern that emerges from our results may be summarized as follows: (a) Mean onset time for detachment = 21.9 ± 0.5 hr LT, (b) the detachment always occurs after the vertical drift has reverted to negative (from Figure 5b the mean time of reversal is 19.4 ± 0.4 hr LT) and before midnight, (c) mean apex height of detachment = 616 ± 56 km, (d) mean time for reconnection to occur is ∼11 min, (e) the detachment and reconnection process occurs between two adjacent bubbles or between the bifurcated branches of the same plasma bubble, and (f) the events occur from September to December for high, medium and low solar flux over Brazilian sector. It is worth mentioning that the airglow images reported by Chian et al. (2018) were obtained on 28 September 2002 in another location in Brazil.

7. Discussion

We intend to offer some statistics on the phenomenon under study. Based on our data, the probability of detachment to occur is 1/121 for 2001, 1/131 for 2004, 1/120 for 2005, 1/130 for 2013, and 1/165 for 2015. This probability is very low compared to the high rate of occurrence of plasma bubbles observed for the period. For example, in the year 2013, there were 130 nights with plasma bubbles, and one single event with a detachment was observed. In the identified events, we did not observe merging between the adjacent bubbles. Based on ionosonde observations over Brazil, the persistence of vertical drift after sunset to show the prereversal and change of direction during many nights, similar to those shown in Figure 5, is greater than the number of days with detachment of bubbles seen by the all-sky imager per year. In our database the high occurrence rate of bubbles observed and the temporal shape of the vertical drift of background suggest that the change of direction of the drift from positive to negative (in the temporary variation) does not contribute to the development of the mechanism proposed by Laakso et al. (1994). Therefore, the factor that could contribute to the effect of opposite vertical drifts inside the bubble must be another, which leads to the supposition that the origin of the detachment must be inside the bubble. On the other hand, the electric fields that develop inside the bubble (E_{in}) are larger compared to the background zonal electric field (E_{out}). For a plasma bubble in its developed phase the electric field E_{in} varies between 0.003 V/m and 0.010 V/m, while the $E_{out} \approx 0.0005$ V/m (Aggson et al., 1996; Carrasco et al., 2020).

On the other hand, the theory proposed by Sahai et al. (2006) including non-homogeneous electric fields requires a simulation code for proper evaluation. The first simulation of detachment was conducted by Yokoyama et al. (2014), using a background zonal electric field positive and constant in time as an input parameter, but the cause of detachment was not discussed in detail because the focus of their work was to study turbulence in plasma bubbles at the equator. We do not know the conditions that control the detachment mechanism and why it occurs only in the last 4 months of the year in the Brazilian sector. We have no explanation for the seasonal occurrence (September–December). The low rate of occurrence of the phenomenon complicates its statistical study. To our knowledge, until now no work in the literature reported disconnection and reconnection between adjacent bubbles using numerical simulation. The simulation by theoretical models can reveal unknown details of the phenomenon under study.

Narayanan, Gurubaran, and Shiokawa (2016) and Narayanan, Gurubaran, Shiokawa, et al. (2016) have shown observations of the phenomenon for January, February, and March in the magnetic northern hemisphere, while our observations of the phenomenon were for September, October, November, and December in the southern

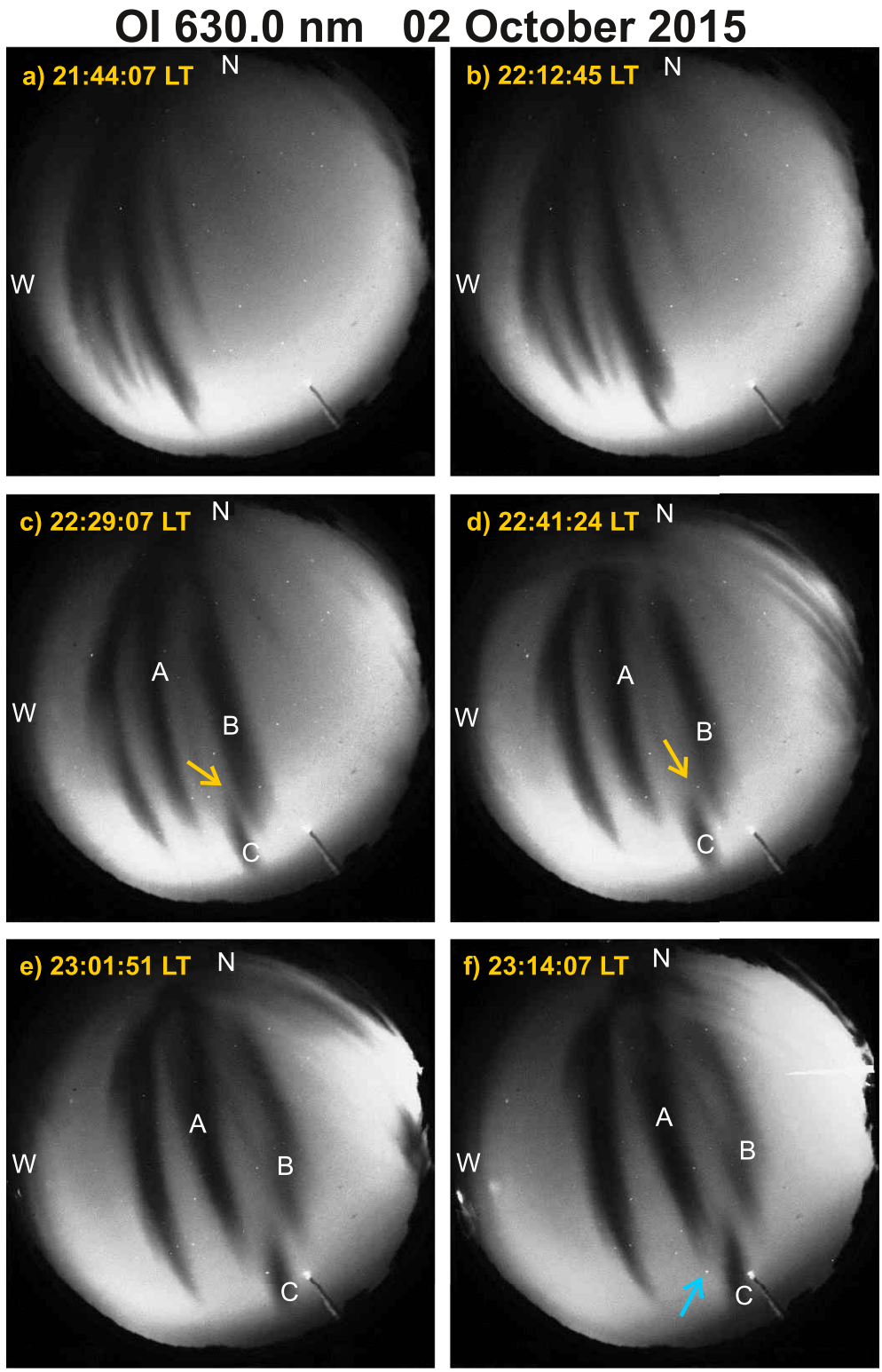

Figure 10. OI 630 nm images from Cariri on 2 October 2015.

Table 1
Events Observed

Day	TimeD (LT)	TimeR (LT)	Apex-height	Ap	F10.7
17/12/2001	22:02:10	22:08:30	588.8	16	206
10/10/2004	21:12:11	21:18:31	600.6	8	89
25/09/2005	21:50:32	21:56:54	550.1	5	81
06/12/2013	21:55:21	22:00:43	642.2	3	151
02/10/2015	22:41:24	23:14:07	697.2	12	107

magnetic hemisphere. These data show that the phenomenon occurs in winter in the northern hemisphere, and spring in the southern hemisphere revealing a seasonal variation that was not addressed in previous studies. So, solar declination can play a role in modulating the phenomenon. On the other hand, this important result must be considered in theoretical models for the simulation of the phenomenon (disconnection-reconnection). The zonal drift velocities of the bubbles calculated in our work are different from those obtained by Narayanan, Gurubaran, and Shiokawa (2016). This result suggests that the phenomenon (disconnection/reconnection) can be independent of the zonal drift velocity of the bubbles. Additionally, in our work, the apex altitude observed varies between 550 and 697 km, and in Narayanan, Gurubaran, and Shiokawa (2016) varies between 280 and 650 km. Narayanan, Gurubaran, Shiokawa, et al. (2016) showed observations of the shrinking of equatorial plasma bubbles, and Narayanan, Gurubaran, and Shiokawa (2016) reported that the merging of equatorial plasma bubbles is facilitated by multiple pathways, which is a different point of view than the one proposed by Huba et al. (2015). The results reported by Narayanan, Gurubaran, and Shiokawa (2016) have allowed increasing the vision of the phenomenon under study. However, the morphological characteristic of shrinking and merging of equatorial plasma bubbles were not observed in our data for the Brazilian sector. We do not know the cause of this dynamic difference between both sectors (India and Brazil). This question that arises from our work suggests continuing in this line of research.

8. Conclusions

Airglow images observations at Cariri/Brazil were used to study the disconnection and reconnection phenomenon in adjacent plasma bubbles. Based on the results obtained, the probability of disconnection and reconnection varies between 1/120 and 1/165 per year. This probability is very low compared to the high rate of plasma bubbles observed each year. We analyzed 2,012 nights with plasma bubbles between 2001 and 2019 and only five events of disconnection/reconnection were found in that period. With only five events available, it was impossible to determine the phenomenon's dependence on geophysical parameters. The phenomenon studied seems to be independent of solar and geomagnetic activity. The observations indicate that the phenomenon can be observed at least between September and December in the southern magnetic hemisphere (Brazil) and between January and March in the northern magnetic hemisphere (India). This first report of the seasonal variation in both hemispheres indicates that the solar declination may play a role in modulating this phenomenon. In the identified events, we did not observe merging between adjacent bubbles over the Brazilian sector. In the future we intend to extend this study to other locations in the Brazilian sector. Understanding the exact mechanism of the pinching or detachment and reconnection requires a more significant effort in theoretical simulation models of electrodynamics of the ionosphere. Additionally, the morphological characteristics of shrinking and merging in equatorial plasma bubbles reported by Narayanan, Gurubaran, and Shiokawa (2016) and Narayanan, Gurubaran, Shiokawa, et al. (2016) were not observed in our data in the Brazilian sector. We suggest continuing this line of research to find an explanation for the difference between the Indian and Brazilian sectors. To conclude, we propose that the hypotheses indicated by Sahai et al. (2006), Laakso et al. (1994) and Gurav et al. (2019) should be examined through theoretical models in plasma bubbles simulation. The simulation by theoretical models could reveal unknown details of the phenomenon under study.

Conflict of Interest

The authors declare no conflicts of interest relevant to this study.

Data Availability Statement

The numerical values (Figures 4 and 5) and the ionospheric data used in this work have been uploaded to a website (http://doi.org/10.5281/zenodo.6419640). The ionospheric data can be visualized using the SAOExplorer software available at https://ulcar.uml.edu/SAO-X/SAO-X.html.

Acknowledgments
The authors wish to acknowledge the support from CAPES-PRINT (process 8887.374260/2019-00) through which the visit of Dr. Carrasco to the National Institute for Space Research—INPE was made possible. ISB acknowledges the support of CNPq under grants 405555/2015-0 and 306844/2019-2. The airglow images of São João do Cariri used in this work can be downloaded upon registration at the Embrace webpage from INPE Space Weather Program at the following link: http://www2.inpe.br/climaespacial/portal/en/.

References

Abdu, M. A., Batista, I. S., Reinisch, B. W., Souza, J. R., Sobral, J. H. A., Pedersen, T. R., et al. (2009). Conjugate point equatorial experiment (COPEX) campaign in Brazil: Electrodynamics highlights on spread F development conditions and day-to-day variability. *Journal of Geophysical Research*, *114*(A04308), 1–21. https://doi.org/10.1029/2008JA013749

Aggson, T. L., Laakso, H., Maynard, N. C., & Pfaff, R. F. (1996). In situ observations of bifurcation of equatorial ionospheric plasma depletions. *Journal of Geophysical Research*, *101*(A3), 5125–5132. https://doi.org/10.1029/95JA03837

Aggson, T. L., Maynard, N. C., Hanson, W. B., & Saba, J. L. (1992). Electric field observations of equatorial bubbles. *Journal of Geophysical Research*, *97*(A3), 2997–3009. https://doi.org/10.1029/90JA02356

Arruda, D. C. S., Sobral, J. H. A., Abdu, M. A., Castilho, V. M., Takahashi, H., Medeiros, A. F., & Buriti, R. A. (2006). Theoretical and experimental zonal drift velocities of the ionospheric plasma bubbles over the Brazilian region. *Advances in Space Research*, *38*(11), 2610–2614. https://doi.org/10.1016/j.asr.2006.05.015

Barros, D., Takahashi, H., Wrasse, C. M., & Figueiredo, C. A. O. B. (2018). Characteristics of equatorial plasma bubbles observed by TEC map based on ground-based GNSS receivers over South America. *Annales Geophysicae*, *36*(1), 91–100. https://doi.org/10.5194/angeo-36-91-2018

Batista, I. S., Abdu, M. A., & Bittencourt, J. A. (1986). Equatorial F region vertical plasma drift: Seasonal and longitudinal asymmetries in the American sector. *Journal of Geophysical Research*, *91*(A11), 12055–12064. https://doi.org/10.1029/JA091iA11p12055

Batista, I. S., Abdu, M. A., Carrasco, A. J., Reinisch, B. W., Paula, E. R., Schuch, N. J., & Bertoni, F. (2008). Equatorial spread F and sporadic E-layer connections during the Brazilian conjugate point equatorial experiment (COPEX). *Journal of Atmospheric and Solar-Terrestrial Physics*, *70*(8–9), 1133–1143. https://doi.org/10.1016/j.jastp.2008.01.007

Bittencourt, J. A., & Abdu, M. A. (1981). A Theoretical comparison between apparent and real vertical ionization drift velocities in the equatorial F region. *Journal of Geophysical Research*, *86*(A4), 2451–2454. https://doi.org/10.1029/JA086iA04p02451

Buriti, R. A., Takahashi, H., & Gobbi, D. (2001). First results from mesospheric airglow observations at 7.5°S. *Revista Brasileira de Geofísica*, *19*(2), 1–7. https://doi.org/10.1590/S0102-261X2001000200005

Carrasco, A., Batista, I. S., & Abdu, M. A. (2014). Numerical simulation of equatorial plasma bubbles over Cachimbo: COPEX campaign. *Advances in Space Research*, *54*(3), 443–445. https://doi.org/10.1016/j.asr.2013.10.017

Carrasco, A. J., Pimenta, A. A., Wrasse, C. M., Batista, I. S., & Takahashi, H. H. (2020). Why do equatorial plasma bubbles bifurcate? *Journal of Geophysical Research: Space Physics*, *125*(11), e2020JA028609. https://doi.org/10.1029/2020JA028609

Chian, A. C. L., Abalde, J. R., Miranda, R. A., Borotto, F. A., Hysell, D. L., Rempel, E. L., & Ruffolo, D. (2018). Multi-spectral optical imaging of the spatiotemporal dynamics of ionospheric intermittent turbulence. *Nature Scientific Reports*, *8*, 1–15. https://doi.org/10.1038/s41598-018-28780-5

Fejer, B. G., Paula, E. R., González, S. A., & Woodman, R. F. (1991). Average vertical and zonal F region plasma drifts over Jicamarca. *Journal of Geophysical Research*, *96*(A8), 13910–13906. https://doi.org/10.1029/91JA01171

Fejer, B. G., Scherliess, L., & Paula, E. R. (1999). Effects of the vertical plasma drift velocity on the generation and evolution of equatorial spread F. *Journal of Geophysical Research*, *104*(A9), 19859–19869. https://doi.org/10.1029/1999JA900271

Gurav, O. B., Narayanan, V. L., Sharma, A. K., Ghodpage, R. N., Gaikwad, H. P., & Patil, P. T. (2019). Airglow imaging observations of some evolutionary aspects of equatorial plasma bubbles from Indian sector. *Advances in Space Research*, *64*(2), 385–399. https://doi.org/10.1016/j.asr.2019.04.008

Heelis, R. A., Kendall, P. C., Moffett, R. J., & Rishbeth, H. (1974). Electrical coupling of the E- and F- regions and its effect on F-region drifts and winds. *Planetary and Space Science*, *22*(5), 743–756. https://doi.org/10.1016/0032-0633(74)90144-5

Huang, C. S., & Kelley, M. C. (1996). Nonlinear evolution of equatorial spread F: Gravity wave seeding of Rayleigh-Taylor instability. *Journal of Geophysical Research*, *101*(A1), 293–302. https://doi.org/10.1029/95JA02210

Huang, C. S., Retterer, J. M., Beaujardiere, O., Roddy, P. A., Hunton, D. E., Ballenthin, J. O., & Pfaff, R. F. (2012). Observations and simulations of formation of broad plasma depletions through merging process. *Journal of Geophysical Research*, *117*(A2), 1–11. https://doi.org/10.1029/2011JA017084

Huba, J. D., Wu, T. W., & Makela, J. J. (2015). Electrostatic reconnection in the ionosphere. *Geophysical Research Letters*, *42*, 1–6. https://doi.org/10.1002/2015GL063187

Laakso, H., Aggson, T. L., Pfaff, R. F., & Hanson, W. B. (1994). Downdrafting plasma flow in equatorial bubbles. *Journal of Geophysical Research*, *99*(A6), 11507–11515. https://doi.org/10.1029/93JA03169

Medeiros, A. F., Buriti, R. A., Machado, E. A., Takahashi, H., Batista, P. P., Gobbi, D., & Taylor, M. J. (2004). Comparison of gravity wave activity observed by airglow imaging at two different latitudes in Brazil. *Journal of Atmospheric and Solar-Terrestrial Physics*, *60*(6–9), 647–654. https://doi.org/10.1016/j.jastp.2004.01.016

Narayanan, V. L., Gurubaran, S., & Shiokawa, K. (2016). Direct observational evidence for the merging of equatorial plasma bubbles. *Journal of Geophysical Research: Space Physics*, *121*(8), 7923–7931. https://doi.org/10.1002/2016JA022861

Narayanan, V. L., Gurubaran, S., Shiokawa, K., & Emperumal, K. (2016). Shrinking equatorial plasma bubble. *Journal of Geophysical Research: Space Physics*, *121*(7), 6924–6935. https://doi.org/10.1002/2016JA022633

Paulino, I., Medeiros, A. F., Vadas, S. L., Wrasse, C. M., Takahashi, H., Buriti, R. A., et al. (2016). Periodic waves in the lower thermosphere observed by OI 630 nm airglow images. *Annales Geophysicae*, *24*(2), 293–301. https://doi.org/10.5194/angeo-34-293-2016

Retterer, J. M. (2010). Forecasting low-latitude radio scintillation with 3-D ionospheric plume models: Plume model. *Journal of Geophysical Research*, *115*(A3), 1–18. https://doi.org/10.1029/2008JA013840

Sahai, Y., Abalde, J. R., Fagundes, P. R., Pillat, V. G., & Bittencourt, J. A. (2006). First observations of detached equatorial ionospheric plasma depletions using OI 630 nm and OI 777.4 nm emissions nightglow imaging. *Geophysical Research Letters*, *33*(11), 1–5. https://doi.org/10.1029/2005GL025262

Scherliess, L., & Feger, B. G. (1999). Radar and Satellite global equatorial F region vertical drift model. *Journal of Geophysical Research*, *104*(A4), 6829–6842. https://doi.org/10.1029/1999JA900025

Sobral, J. H. A., Abdu, M. A., Pedersen, T. R., Castilho, V. M., Arruda, D. C. S., Muella, M. T. A. H., et al. (2009). Ionospheric zonal velocities at conjugate points over Brazil during the COPEX campaign: Experimental observations and theoretical validations. *Journal of Geophysical Research*, *114*(A04309), 1–24. https://doi.org/10.1029/2008JA013896

Takahashi, H., Lima, L. M., Wrasse, C. M., Abdu, M. A., Batista, I. S., Gobbi, D., et al. (2005). Evidence on 2−4 day oscillations of the equatorial ionosphere h′F and mesospheric airglow emissions. *Geophysical Research Letters*, *32*(12), 1–4. https://doi.org/10.1029/2004GL022318

Takahashi, H., Wrasse, C. M., Otsuka, Y., Ivo, A., Gomes, V., Paulino, I., et al. (2015). Plasma bubble monitoring by TEC map and 630 nm airglow image. *Journal of Atmospheric and Solar-Terrestrial Physics*, *130*, 151–158. https://doi.org/10.1016/j.jastp.2015.06.003

Wrasse, C. M., Nakamura, T., Takahashi, H., Medeiros, A. F., Taylor, M. J., Gobbi, D., et al. (2006). Mesospheric gravity waves observed near equatorial and low-middle latitude stations: Wave characteristics and reverse ray tracing results. *Annales Geophysicae*, *24*(12), 3229–3240. https://doi.org/10.5194/angeo-24-3229-2006

Yokoyama, T., Shinagawa, H., & Jin, H. (2014). Nonlinear growth, bifurcation, and pinching of equatorial plasma bubble simulated by three-dimensional high-resolution bubble model. *Journal of Geophysical Research*, *119*(12), 10474–10482. https://doi.org/10.1002/2014JA020708